ORIGINAL RESEARCH

Dioscin Ameliorates Experimental Autoimmune Thyroiditis via the mTOR and TLR4/NF-κB Signaling

Chengfei Zhang [1,2,*], Qiue Zhang [3,*], Lingling Qin [4,*], Zhiyi Yan [5], Lili Wu [4,5], Tonghua Liu [5]

[1]School of Life Sciences, Beijing University of Chinese Medicine, Beijing, People's Republic of China; [2]Dongfang Hospital of Beijing University of Chinese Medicine, Beijing, People's Republic of China; [3]School of Traditional Chinese Medicine, Beijing University of Chinese Medicine, Beijing, People's Republic of China; [4]Technology Department, Beijing University of Chinese Medicine, Beijing, People's Republic of China; [5]Key Laboratory of Health Cultivation of the Ministry of Education, Beijing University of Chinese Medicine, Beijing, People's Republic of China

*These authors contributed equally to this work

Correspondence: Tonghua Liu, Key Laboratory of Health Cultivation of the Ministry of Education, Beijing University of Chinese Medicine, Beijing, People's Republic of China, Email thliu@vip.163.com

Background: Autoimmune thyroiditis (AIT) is a common autoimmune disease that causes thyroid dysfunction. Clinical symptoms in Hashimoto thyroiditis patients were improved after oral administration of dioscin. However, the mechanisms involved in the therapeutic effect remain unclear.

Methods: The protective effects and potential mechanisms of dioscin for autoimmune thyroiditis were explored in a rat model of thyroglobulin-induced autoimmune thyroiditis. Firstly, the rat model of AIT was obtained by subcutaneous injection of thyroglobulin and drinking the sodium iodide solution, followed by gavage administration for 8 weeks. Rats were sacrificed after anaesthesia, serum and thyroid samples were preserved. Serum triiodothyronine (T3), thyroxine (T4), free triiodothyronine (FT3), free thyroxine (FT4), thyrotropin (TSH), thyroglobulin antibody (TgAb), thyroid peroxidase antibody (TPOAb), and thyrotropin receptor antibody (TRAb) expressions were measured by enzyme-linked immunosorbent assay (ELISA). Morphological changes were observed by H&E staining. Next, we used transcriptomics techniques to find the potential therapeutic target of dioscin. Finally, we validated the transcriptomic results by reverse transcription-polymerase chain reaction (RT-PCR) and immunohistochemistry (IHC-P), respectively.

Results: Animal experiments showed that dioscin regulated T3, T4, FT3, TSH, TgAb, TPOAb, and TRAb and alleviated the pathological process in a dose-dependent manner, with the high-dose group showing optimal efficacy. In the transcriptome, the nuclear factor kappa B (NF-κB) pathway was identified by KEGG enrichment analysis and validated by RT-PCR and IHC-P. The relative expression of NF-κB, mechanistic target of rapamycin (mTOR), and toll-like receptor 4 (TLR4) mRNA and protein were decreased in the dioscin-treated group compared to the AIT model group.

Conclusion: Our results suggest that dioscin treatment improved thyroid function and downregulated TGAb, TPOAb and TRAb levels in rat models of AIT, which may alleviate the pathological process and suppress the inflammatory response by inhibiting mTOR and TLR4/NF-κB pathways.

Keywords: dioscin, autoimmune thyroiditis, transcriptome, TLR4/NF-κB

Introduction

Autoimmune thyroiditis refers to an organ-specific autoimmune disease characterised by structural destruction of thyroid tissue and hypothyroidism caused by lymphocyte-infiltrating autoantibodies (TPOAb and TgAb) in the thyroid tissue.[1] High titers of TgAb are present in most patients with AIT (40%-70%), and more than 80% of patients with AIT have high titers of TPOAb.[2] In general, the diagnosis can be confirmed by thyroid ultrasound and antibody testing in clinical practice. The prevalence of AIT is increasing year by year and is much higher in women than in men.[3]

The pathogenesis of AIT is unclear and may be related to genetic susceptibility, environmental factors, and endogenous factors. Their interaction leads to the destruction of immune tolerance, the production of thyroid autoantigens and to the subsequent activation of T lymphocytes, which induce lymphocyte migration to the thyroid and produce

Graphical Abstract
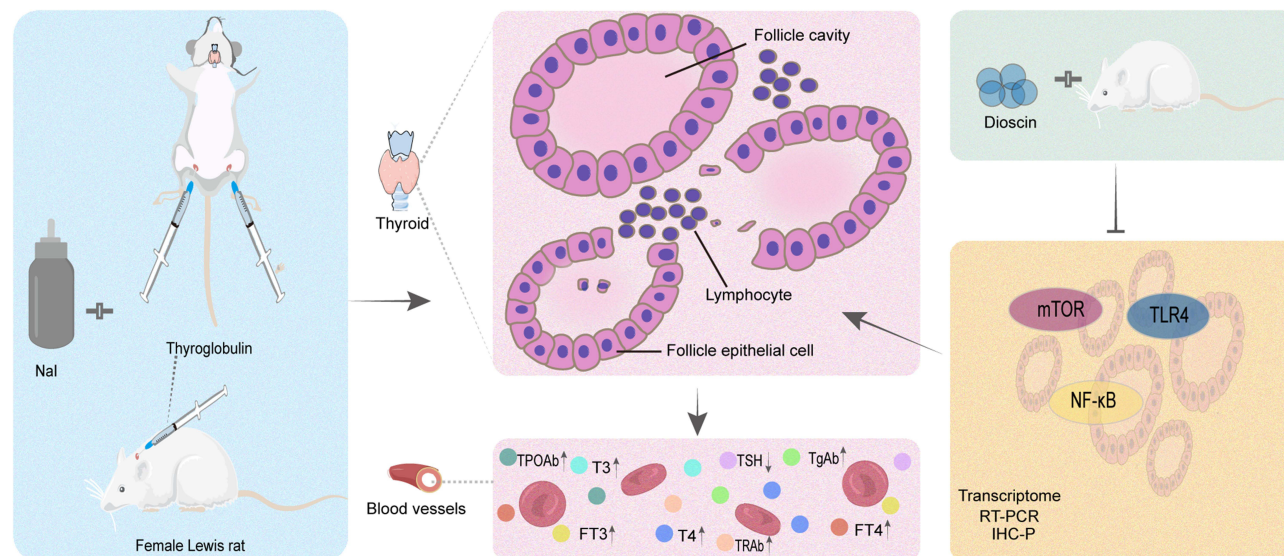
anti-thyroid autoantibodies.[4] Currently, there are no specific treatment options for AIT, which are limited and carry a high risk of serious side effects, including surgical treatment, thyroid hormone therapy or immunomodulatory therapy. Therefore, there is an urgent need to find a new effective and safe drug for AIT.

Dioscin is a natural steroidal saponin extracted from the roots of the *Dioscorea* plants, *Dioscorea nipponica* and *Dioscorea zingiberensis*.[5] In recent years, the anti-inflammatory, immunomodulatory, antiallergic, antifungal, and antiviral effects of dioscin have attracted increasing attention due to its effective role in the treatment of brain, liver, kidney, stomach, and intestinal injuries, and metabolic diseases such as obesity, diabetes, hyperuricemia, and osteoporosis.[6] Dioscin exerts good anti-inflammatory effects.[7] Clinical symptoms were improved after oral administration of dioscin.[8] Further experiments on animal and cellular mechanisms revealed that dioscin can promote the differentiation of the $CD4^+CD25^+Foxp3^+$ Treg cells and subsequently upregulate the SUMOylation of interferon regulatory factor 4 by downregulating the expression of SUMO specific peptidase 1. However, there are limitations to the previous hypothetical research. To fully understand the therapeutic effects and molecular mechanisms of dioscin activity, transcriptome sequencing was used to investigate the effects of dioscin on gene expression in the thyroid tissue from AIT rats. The overall aim of this study was to observe the protective effects of dioscin in the rat model of AIT and to explore the possible mechanism of action involved.

Materials and Methods

Animals

Four-week-old female specific pathogen-free (SPF) Lewis rats (80 ± 10 g) were purchased from Beijing Vital River Laboratory Animal Technology Co. (License No. SCXK, Beijing, 2016–0006). The rats were housed in the laboratory of the Experimental Animal Center of Beijing University of Traditional Chinese Medicine [No. SYXK (Jing) 2020–0033] under SPF conditions in a temperature -controlled breeding room with a 12 h:12 h light-dark cycle. All experimental procedures were approved by the Laboratory Animal Ethics Committee of Beijing University of Chinese Medicine (No. BUCM-4-2019070303-3003.).

Reagents

Dioscin (high performance liquid chromatography [HPLC] ≥98%, lot: Y20A10Z95575, Shanghai Yuanye Bio-Technology Co., Ltd, Shanghai, China, chemical structure shown in Figure 1A was dissolved in 0.5% CM cellulose
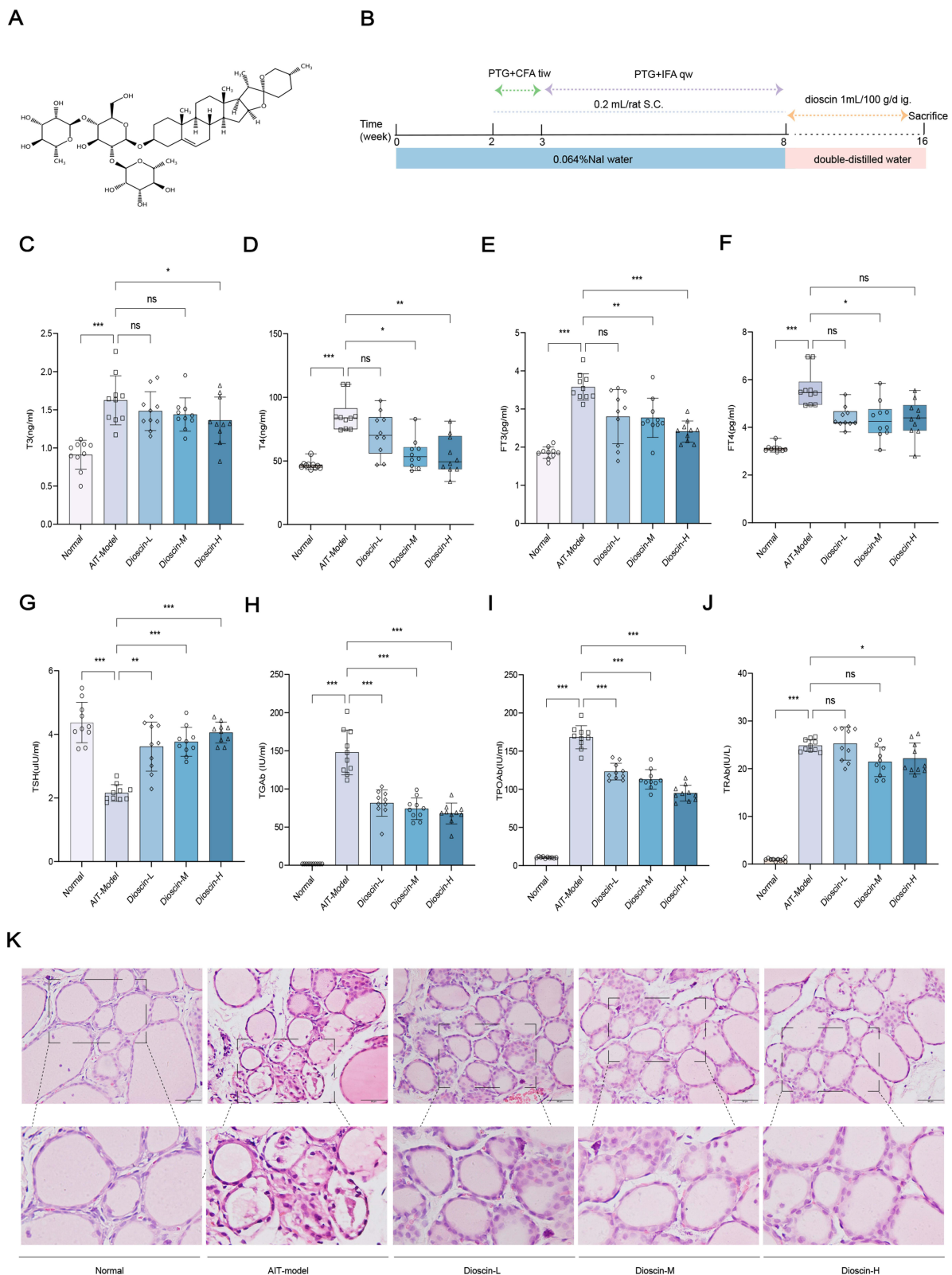
Figure 1 Dioscin attenuates thyroid dysfunction and inflammatory infiltration in Lewis rats. (**A**) The chemical structure of dioscin. (**B**) Autoimmune thyroiditis induction and dioscin administration scheme. (**C–J**) Serum results of thyroid function, TGAb, TPOAb and TRAb. (n =10). *$P < 0.05$, **$P < 0.01$, ***$P < 0.001$, ns= $P > 0.05$.

sodium salt solution (lot: SL29151602, Coolaber, Beijing, China) and added to 0.02% dimethyl sulfoxide (lot: 1129E031, Solarbio, Beijing, China) to prepare the suspension for in vivo studies.

Sodium iodide was prepared as a 0.064% solution using deionized water as the solvent and stored in tin foil wrapped away from light (NaI, CAS No. 7681-82-5, 99% AR, Maya-R). The emulsifier was prepared as follows: porcine thyroglobulin (PTg) was dissolved in phosphate buffered saline to make a 0.1% solution, then mixed with Freund's complete adjuvant (CFA) in a 1:1 volume ratio and emulsified. The final concentration of PTg was 0.05%. Freund's incomplete adjuvant (IFA) was prepared similarly to the CFA solution (lot. SLBW7430, SIGMA, St. Louis, MO, USA; IFA, lot. SLBZ0619, Sigma; PTg, lot.018K7012, SIGMA).

AIT Induction in Rats and Drug Treatment

Ten rats were randomly selected as the normal group, and the rest were subjected to the AIT model (Figure 1B). To induce the AIT animal model,[9] from the first week of the experiment, the rats were allowed to drink 0.064% NaI freely, while the non-model control rats were allowed to drink double-distilled water freely. In the third week, the model rats were immunized for the first time: thyroid globulin emulsion with Freund's complete adjuvant was injected subcutaneously into the paw pad, back, and neck of the rats at multiple sites at 0.2 mL each. Two injections were given 2 days apart in one week. Enhanced immunization: 0.2 mL was injected into the paw pad, subcutaneous back, and subcutaneous neck of rats from week 4 to week 8. To verify the success of the model development, blood samples were collected from the orbital vein, and the level of TPOAb antibody in peripheral serum was detected by ELISA. Serum TPOAb concentration in the model group is at least 10 times that of the normal group. In this study, before administration, the serum TPOAb (IU/mL) concentration of the model rats was 178.682±11.160 and that of the normal group was 9.347 ±0.839. The TPOAb in model rats was 19.117 times that of normal rats, and it is considered that the model is successful. Three model rats were randomly selected for histologic evaluation of thyroid changes. Rats were grouped before drug administration with no statistically significant difference in TPOAb levels between the groups.

Fifty rats were randomly divided into the normal group (control), AIT-model group, dioscin low-dose group, dioscin middle-dose group, dioscin high-dose group, with 10 rats in each group. After the AIT model was achieved, rats in the dioscin low-dose (dioscin-L) group (25 mg/kg/d), dioscin middle-dose (dioscin-M) group (50 mg/kg/d) and dioscin high-dose (dioscin-H) group (100 mg/kg/d) were given the corresponding drug suspensions, and rats in the normal (control) group and the model group were given the same volume of deionized water,1 mL/100 g/d, continuously for 8 weeks.

The dioscin-H treatment group was evaluated by transcriptome, RT-PCR and IHC-P analysis. The dioscin-L and dioscin-M groups were excluded due to better efficacy of the high dose.

Serum and Histology Examination

After the treatments, the rats were anesthetized with 1% pentobarbital sodium, and blood was collected from the abdominal aorta to obtain serum. T3, T4, FT3, FT4, TSH, TGAb and TRAb were detected by Beijing Sino-UK Institute of Biological Technology. The expression level of TPOAb was detected by ELISA (TPOAb ELISA Kit, lot: C0336030355, CUSABIO, Wuhan, China). One unilateral thyroid gland was excised and fixed in 4% paraformaldehyde for pathological observation, while the contralateral thyroid gland was immediately placed in liquid nitrogen for transcriptome, RT- PCR and IHC-P.

Transcriptome Sequencing

Transcriptome sequencing and analysis were performed by OE biotech Co., Ltd. (Shanghai, China).

RNA Extraction and Library Preparation

Total RNA was extracted using the mirVana miRNA Isolation Kit (Ambion, Austin, TX, USA) according to the manufacturer's protocol. RNA integrity was assessed using the Agilent 2100 Bioanalyzer (Agilent Technologies, Santa Clara, CA, USA). Samples with an RNA Integrity Number (RIN) ≥ 7 were subjected to library preparation using the TruSeq Stranded mRNA LTSample Prep Kit (Illumina, San Diego, CA, USA) according to the manufacturer's

instructions. These libraries were then sequenced on the Illumina sequencing platform (HiSeqTM 2500 or Illumina HiSeq X Ten) and 125bp/150bp paired-end reads were generated.

Bioinformatics Analysis
Quality Control and Mapping
The raw data (raw reads) were processed using Trimmomatic.[10] The reads containing ploy-N and the low quality reads were removed to obtain the clean reads, which were then mapped to the reference genome using hisat2.[11]

Gene-Level Quantification, Analysis of Differentially Expressed Genes, Cluster Analysis, GO, and KEGG Enrichment
The FPKM, or Fragments Per kilobase of transcript Per Million mapped Reads,[12] value of each gene was calculated using cufflinks,[13] and the read counts of each gene were obtained using htseq-count.[14] Differentially expressed genes (DEGs) were identified using the DESeq[15] R package functions estimate SizeFactors and nbinomTest. A P-value <0.05 and foldChange >2 or foldChange <0.5 were set as the thresholds for significant differential expression. Hierarchical cluster analysis of DEGs was performed to explore gene expression patterns. GO enrichment and KEGG[16] pathway enrichment analysis of DEGs were respectively performed using R, based on the hypergeometric distribution.

Transcript-Level Quantification, Analysis of Differentially Expressed Transcript, Cluster Analysis, GO and KEGG Enrichment
Transcript-level quantification, FPKM, and read count values for each transcript (protein_coding) were calculated using bowtie2[17] and eXpress.[18] DEGs analysis was the same as above: 2.5.2.2.

Real-Time Quantitative RT-PCR
RNA extraction and real-time quantitative reverse transcription (RT)-PCR were conducted by OE biotech Co., Ltd. (Shanghai, China). Quantification was performed with a two-step reaction process: RT and PCR. Each RT reaction consisted of 0.5 μg RNA, 2 μL of 5×TransScript All-in-one SuperMix for qPCR and 0.5 μL of gDNA Remover, in a total volume of 10 μL. Reactions were performed on a GeneAmp PCR System 9700 (Applied Biosystems, Foster City, CA, USA) for 15 min at 42°C and 5 s at 85°C. The 10 μL RT reaction mix was then diluted 10-fold in nuclease-free water and stored at −20°C. Real-time PCR was performed using the LightCycler 480 II Real-time PCR Instrument (Roche, Basel, Switzerland) with 10 μL PCR reaction mixture containing 1μL of cDNA, 5 μL of 2×PerfectStartTM Green qPCR SuperMix, 0.2 μL of forward primer, 0.2 μL of reverse primer, and 3.6 μL of nuclease-free water. Reactions were incubated in a 384-well optical plate (Roche) at 94°C for 30s, followed by 45 cycles of 94°C for 5s and 60°C for 30s. Each sample was run in triplicate for analysis. At the end of the PCR cycles, melting curve analysis was performed to validate the specific generation of the expected PCR product. Primer sequences were designed in the laboratory and synthesized by TsingKe Biotech based on the mRNA sequences obtained from the NCBI database as follows: AdipoR (102 bp) Forward primer (5→3): CCCTGGCTCTATTACTCCTT, Reverse primer (5→3): CCACTGTGCCACAATGAT; AMPK (82bp) Forward primer (5→3): TCTATGAACTGGAGGAGCACA, Reverse primer (5→3): GAAATGCAGACAAGTGGCTTA; CREB (105 bp) Forward primer (5→3): CGCAGGTCCATCAGTTACA, Reverse primer (5→3): GGATGA TGAGAGCCAACGA; Leptin (85bp) Forward primer (5→3): TTGGTCCTATCTGTCCTATGTT, Reverse primer (5→3): GGTGACAATGGTCTTGATGAG; PGC-1a (83bp) Forward primer (5→3): GAAATTGAGGAATGCACCGTA, Reverse primer (5→3): AAAGCGTCACAGGTGTAAC; TLR4 (102bp) Forward primer (5→3): GACATGGCAGTTTCTGAGTAG, Reverse primer (5→3): AGAAGGCGATACAATTCGAC; NF-κB (93bp) Forward primer (5→3): TCCAGTG TGTGAAGAAGCGA, Reverse primer (5→3): GCTGCTCCTCTATGGGAAC; mTOR (100 bp) Forward primer (5→3): AAGTTCAGCCCTTCTTTGAC, Reverse primer (5→3): AGAATCAGACAGGCACGA; β-actin (72 bp) Forward primer (5→3): GCGAGTACAACCTTCTTGC, Reverse primer (5→3): TATCGTCATCCATGGCGAAC. The expression levels of mRNAs were normalized to β-actin and were calculated using the $2^{-\Delta\Delta Ct}$ method.

Immunohistochemistry
The main steps of immunohistochemical detection included dewaxing, hydration, 3% hydrogen peroxide treatment, high temperature antigen retrieval, goat serum sealing, primary antibody 4°C overnight, rewarming PBS wash, secondary

antibody drop, DAB color development, hematoxylin staining, hydrochloric acid and alcohol differentiation, tap water wash, dehydration, and sealing. Images were captured under a microscope, and the Image-Pro Plus 6.0, Media Cybernetics system was used to detect absorbance and determine integrated option density (IOD)/area of TLR4 (ab22048, Abcam, Cambridge, MA, USA), NF-κB p65 (ab16502, Abcam), or mTOR (ab32028, Abcam), and to perform statistical processing.

Statistical Analysis

Statistical analysis was carried out using SPSS 20.0 statistical software (SPSS Inc., USA). When the sample size is greater than or equal to 10, we use the Shapiro–Wilk test to assess the normality of the data. When the sample size is less than 10, we employed Q-Q plots for a visual assessment of normality.[19] Mean ±standard deviation (SD) was reported for normally distributed data, while median (quartile 25%, 75%) [M (Q1, Q3)] was used for non-normally distributed data. The Student's t-test was employed for comparing normally distributed data between two groups, and one-way analysis of variance (ANOVA) followed by the least significant difference (LSD) test for groups with equal variances or Dunnett's T3 test for groups with unequal variances was used for three or more groups. Non-normally distributed data was compared using the Mann–Whitney U-test for two groups and the nonparametric Kruskal–Wallis test for three or more groups. Statistical significance was determined by a P-value of less than 0.05.

Results

Serum Expression of Thyroid Function

Compared with the normal group, the levels of T3 (Dunnett's T3 test, $P<0.001$), T4 (Kruskal–Wallis test, $P<0.001$), FT3 (Dunnett's T3 test, $P<0.001$), and FT4 (Kruskal–Wallis test, $P<0.001$) in the model group increased significantly, while the levels of TSH decreased (Dunnett's T3 test, $P<0.001$). Compared with the model group, the concentrations of T3 in the dioscin-H (Dunnett's T3 test, P=0.030), T4 in the dioscin-M (Kruskal–Wallis test, $P=0.047$) and dioscin-H (Kruskal–Wallis test, $P=0.003$) groups decreased. The concentrations of FT3 in the dioscin-M (Dunnett's T3 test, $P=0.008$) and dioscin-H (Dunnett's T3 test, $P<0.001$), and FT4 in the dioscin-M (Kruskal–Wallis test, $P=0.011$) groups decreased. The TSH in the dioscin-L (Dunnett's T3 test, $P=0.001$), dioscin-M (Dunnett's T3 test, $P<0.001$), and dioscin-H (Dunnett's T3 test, $P<0.001$) levels increased significantly (Figure 1C-G).

Thyroid Serum Antibody Expression

Compared with the normal group, TGAb, TRAb and TPOAb in the model group increased significantly (Dunnett's T3 test, $P<0.001$). Compared with the model group, the concentrations of TGAb in the dioscin-L (Dunnett's T3 test, $P<0.001$), dioscin-M (Dunnett's T3 test, $P<0.001$) and dioscin-H (Dunnett's T3 test, $P<0.001$), TPOAb in the dioscin-L (Dunnett's T3 test, $P<0.001$), dioscin-M (Dunnett's T3 test, $P<0.001$) and dioscin-H (Dunnett's T3 test, $P<0.001$), and TRAb in the dioscin-H-treated (Dunnett's T3 test, $P=0.032$) groups were significantly reduced (Figure 1H-J).

Pathological Changes in Thyroid Tissue

In the normal group, a large number of intact thyroid follicles were observed microscopically, with moderate size, uniform presence of red colloids, and intact follicular epithelial cells. In the model group, a diffuse lymphocytic infiltration was observed in the stroma of the thyroid follicles, a large number of follicular lumens were destroyed or reduced, the colloid content in the lumens was unevenly distributed or reduced, and the walls of the follicles were thin and ruptured. Compared with the model group, the lymphocyte infiltration in the thyroid follicular stroma was significantly reduced in the treatment group, the follicular epithelial cells were more intact, and the colloid content was slightly decreased, and the follicular structure was found to be intact. The high-dose group performed better. (Figure 1K).

Analysis of Differentially Expressed Genes

Screening and Expression Level Analysis of DEGs

The DESeq software revealed that the number of differentially expressed genes in the dioscin-treated group was 189, with 179 genes upregulated and 10 downregulated genes compared to the AIT-model group (Figure 2A).

KEGG Enrichment Analysis of DEGs

The distribution of the differentially expressed genes and all genes in the KEGG Level in the dioscin treatment group were compared with those of the AIT-model group (Figure 2B). The bubble diagram of the top 20 KEGG pathways from the enrichment analysis (obtained by selecting pathway entries including 2 or more different genes, and sorted according to the $-\log_{10}P$ value corresponding to each entry from large to small) is shown in Figure 2C.

Based on the pathways correlated with thyroid disease, the AMPK signaling pathway and the NF-kappa B signaling pathway were selected from the KEGG enrichment analysis. The expression of AdipoR, AMPK, PGC-1α, CREB, and leptin mRNA belonging to the AMPK signaling pathway were verified by RT-PCR. The expression of TLR4, NF-κB, and mTOR mRNA was verified by RT-PCR and the relative protein expression was detected by IHC-P.

Real-Time Quantitative RT-PCR

Compared with the AIT group, the relative expression of AdipoR (Mann–Whitney test, $P=0.017$), AMPK (Unpaired t test, $P=0.022$), leptin (Mann–Whitney test, $P=0.960$), PGC-1a (Mann–Whitney test, $P=0.142$), NF-κB (Mann–Whitney test, $P=0.039$), mTOR (Unpaired t test, $P=0.029$), and TLR4 (Unpaired t test, $P=0.089$) mRNA decreased in the dioscin-treatment group, while the relative expression of CREB (Unpaired t test, $P=0.074$) mRNA increased (Figure 3A).

Immunohistochemical Analysis

TLR4 and mTOR immunoreactive signals (brown staining) in thyroid tissue were located in thyroid follicles and follicular stroma using 400× light microscopy, suggesting that TLR4 and mTOR proteins are expressed in thyroid follicles and in the follicular stroma of the thyroid. The NF-κB immunoreactive signals (in brown) were located in the nuclei of thyroid follicular epithelial cells, indicating that NF-κB protein was expressed in the nucleus of thyroid follicular epithelial cells.

Comparing the IOD/Area of each region of interest for each treatment group with the normal group, the expression of TLR4 (Dunnett's T3 test, $P<0.001$), mTOR (Kruskal–Wallis test, $P<0.001$), and NF-κB (Kruskal–Wallis test, $P<0.001$) protein was higher in the thyroid tissue of rats in the AIT model group. Compared with the AIT model group, the expression of TLR4 (Dunnett's T3 test, $P<0.001$), mTOR (Kruskal–Wallis test, $P=0.049$), and NF-κB (Kruskal–Wallis test, $P=0.049$) protein was significantly decreased in the dioscin-treated group (Figure 3B-G).

Discussion

Since AIT is predominant in females, female Lewis rats, which are inbred, highly homogeneous, susceptible to autoimmune diseases, and have good reproducibility, were selected for modeling in this study.[20] An animal model of AIT was established by drinking 0.064% sodium iodide combined with subcutaneous injection of porcine thyroglobulin in rats. Serologic results showed that the titers of serum TGAb, TPOAb and TRAb were significantly higher in the AIT model group than in the normal group. Morphological observation of randomly selected model rats showed that a large number of follicular lumens in the thyroid tissue of the AIT model group were destroyed or reduced, and the luminal colloid content was uneven or reduced with lymphocyte infiltration. In addition, this modeling method has demonstrated its effectiveness and good stability in several other research studies.[21–23] These studies have shown consistent serological and pathological results with the present study, with elevated thyroid autoantibodies, thyroid follicular destruction, and significant infiltration of lymphocytes in the thyroid gland being the key indicators of a successful model.

Compared with the normal group, the serum levels of T3, T4, FT3, and FT4 were significantly increased and the levels of TSH were decreased in the AIT model group, indicating the continued destruction of the thyroid gland, leading to thyrotoxicosis. Serum hormone levels of T3, T4, FT3, FT4, TSH, and thyroid antibodies TgAb, TPOAb and TRAb
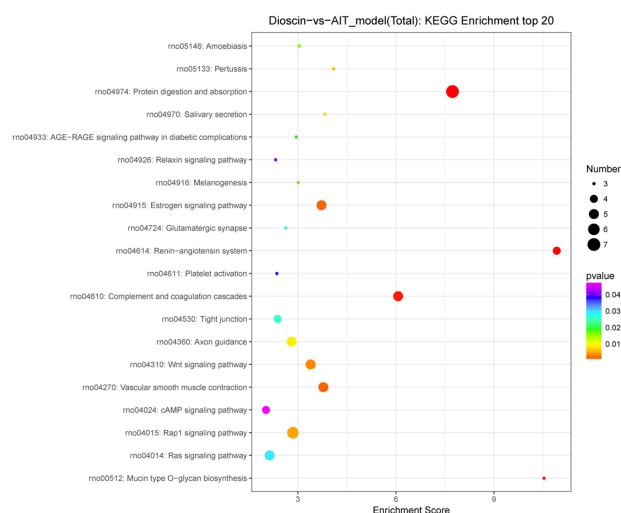
A
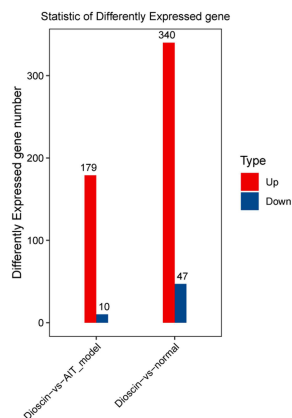
B
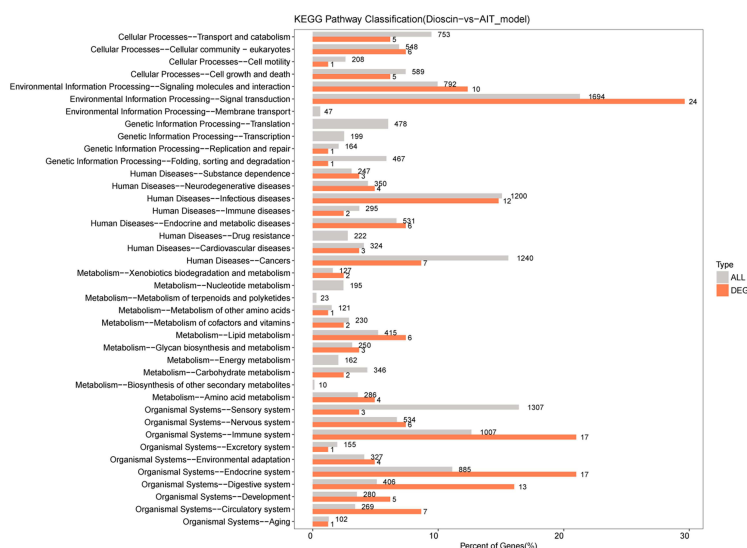
C

Figure 2 (**A**)Statistical histogram of differentially expressed genes. The horizontal axis is each comparison group; The vertical axis is the number of different genes in the comparison group, where up is the number of significantly different up-regulated genes and down is the number of significantly different down-regulated genes. (**B**) Comparison of differentially expressed genes and horizontal distribution of all genes in KEGG Levels. The horizontal axis is the ratio (%) of the total number of genes annotated to each metabolic pathway (differentially expressed genes) and all genes annotated to the KEGG pathway (differentially expressed genes), the vertical axis represents the name of the pathway, and the number on the right side of the column represents the number of differentially expressed genes annotated to this Levels pathway. (**C**) Bubble diagram of top 20 enrichment by KEGG. The X axis in the figure is the enrichment score. The larger the bubble, the higher the number of differential protein coding genes. The color of the bubble changes from purple-blue-green-red. The smaller the enrichment *p*-value, the higher the significance.
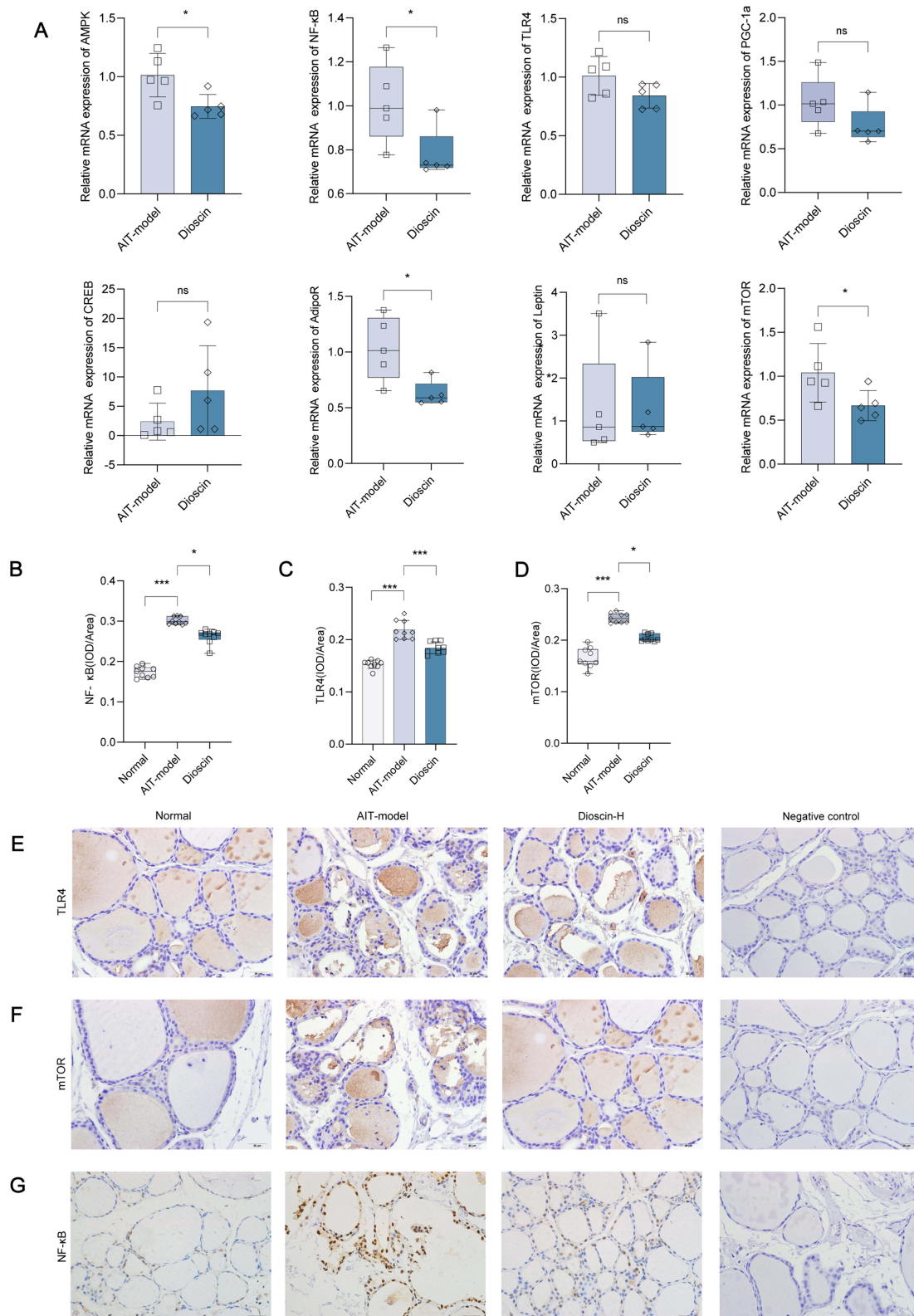
Figure 3 (A) Comparison of mRNA expression in thyroid tissue (n =5). (**B–D**) The results of quantitative analysis of immunohistochemical staining using Image Pro-Plus 6.0 software (n=9). (**E–G**) TLR4, mTOR and NF-κB protein levels in thyroid tissues shown by immunohistochemical staining. *$P < 0.05$, ***$P < 0.001$, ns= $P > 0.05$.

were slightly improved in the dioscin-L and dioscin-M groups after 8 weeks of oral dioscin administration compared with the AIT model group, but the difference was not statistically significant, indicating that dioscin concentrations in these two groups were not sufficient to treat AIT. In contrast, serologic tests in the high-dose group revealed a significant improvement in thyroid function compared to the AIT model group. Pathological results also showed that the high-dose group had less lymphocyte infiltration in the interstitial thyroid follicles and a more intact thyroid structure. Therefore, thyroid tissues from the dioscin-H group of rats were selected for transcriptomic analysis and subsequent validation, with the aim of understanding the potential molecular mechanisms underlying the therapeutic effects of dioscin in AIT rats.

The present study demonstrates that dioscin may have a potential therapeutic effect on AIT in female Lewis rats. Previous studies have investigated the efficacy of various treatments on animal models of AIT. Guo et al's[23] study examined the effect of Prunella vulgaris L. on AIT in rats and found that it significantly reduced TgAb levels and thyroid inflammation scores in experimental autoimmune thyroiditis rats compared to the AIT model group. Similarly, Yang et al[24] showed that high doses of Isaria felina significantly reduced serum TSH, TGAb, and TPOAb levels in AIT mice. Our findings are consistent with these studies, suggesting that dioscin may be a potential therapeutic option for treating AIT. It is important to note that optimal dosages and efficacy of each treatment may vary, and the mechanisms of therapeutic action may also differ. Therefore, further research is necessary to determine the optimal treatments and dosages for animal models and human AIT.

Knowing that the thyroid gland is small and easily degraded, we tried to optimize the experimental design to use as few animals as possible and reduce animal injury. We obtained thyroid tissue and extracted RNA from 5 rats each from normal rats, the AIT model group and the dioscin high-dose group. Overall, DESeq software showed that the number of differentially expressed genes in the dioscin treated group was 189, with 179 genes up-regulated and 10 gens down-regulated compared with the AIT-model group, indicating that dioscin activated numerous genes with widely different functions to alleviate AIT-induced damage. The differentially expressed genes were analyzed by KEGG enrichment. We selected the AMPK and NF-kappa B signaling pathways for RT-PCR verification of the KEGG enrichment analysis based on the correlation of these pathways with thyroid disease. The expression of AdipoR, AMPK, PGC-1α, and leptin in the AMPK signaling pathway were all downregulated in the RT-PCR results, which was contrary to the upregulation revealed by the transcriptome results, so this pathway was excluded. RT-PCR verified two core genes TLR4 and NF-κB in the NF-kappa B signaling pathway and the expression of mTOR mRNA. Compared with the AIT-model group, the relative expression of mTOR (Unpaired t test, $P=0.029$) and NF-κB (Mann–Whitney test, $P=0.039$) mRNA decreased, while TLR4 mRNA decreased, although the differences were not significantly different. In addition, the relative expression of CREB mRNA increased in the dioscin-treated group, but not significantly.

TLR4 plays an important role in the pathogenesis of AIT disease.[25] In Hashimoto's thyroiditis patients, the expression of serum TLR4 is higher than that of unaffected individuals, and TLR4 plays an important role in the immunopathological mechanisms of the disease by inducing a pro-inflammatory response.[26] In this study, TLR4 mRNA (Unpaired t test, $P=0.089$) and the TLR4 IOD/Area (Dunnett's T3 test, $P<0.001$) were downregulated in the dioscin-treated group, suggesting that dioscin could inhibit the inflammatory response in thyroid tissue through TLR4. After activation of the TLR family proteins, the downstream signal transduction pathway is activated, resulting in a complex signal cascade amplification response. NF-κB is an important downstream molecule regulated by TLR4.[27] After activation, it can induce the synthesis and release of various inflammatory mediators, which can further activate innate immune cells and the adaptive immune system.[28] Therefore, NF-kB plays an important role in both the inflammatory and immune responses.[29] Inhibition of NF-κB activity plays an important role in the treatment of AIT. For example, agents such as DHA, which inhibit the phosphorylation of the PI3K/AKT pathway and inhibit the expression of p-NF-κB, and have been proposed as a useful drugs for the treatment of AIT.[30] In this study, TLR4, NF-κB mRNA, and the corresponding IOD/Area in the IHC analysis were downregulated (Kruskal–Wallis test, $P<0.001$), suggesting that dioscin may play a role in the treatment of AIT by inhibiting the TLR4/NF-κB signaling pathway.

mTOR is widely involved in the regulation of cell growth, proliferation, autophagy, and apoptosis of cells, and has been defined as a "central regulator" of cellular activity.[31] The mTOR signaling pathway may regulate autophagy and cell proliferation in the thyroiditis model.[32] Compared with the AIT-model group, mTOR mRNA (Unpaired t test, $P=0.029$) and the relative IOD/Area (Kruskal–Wallis test, $P<0.001$) were down-regulated in the dioscin group. Dioscin may inhibit

mTOR expression, inhibit cell proliferation, and induce autophagy to some extent. The downregulation of AMPK expression assessed by RT-PCR suggested that mTOR was not activated by AMPK. In the KEGG enrichment analysis, the PI3K-Akt signaling pathway was upregulated, suggesting that mTOR might not be downregulated by inhibition of the PI3K-Akt pathway. How dioscin affects the regulation of mTOR deserves further study. In addition, mTOR regulates the pro-inflammatory immune response by regulating transcription factors including NF-κB.[33] It has been suggested that dioscin may attenuate the inflammatory immune response not only by inhibiting the TLR4/NF-κB signaling pathway, but also by inhibiting the mTOR/NF-κB pathway.

Apoptosis is the main mechanism of thyroid cell death.[34] In Graves' disease, there are three thyroid stimulating hormone receptor antibodies with different functions (stimulating, blocking, and cleaving). The stimulating antibody can induce the survival and proliferation of thyroid cells through the cAMP/PKA/CREB pathway, while the cleavage antibody can induce cell death through mitochondrial ROS (mROS), and the generation of cAMP/PKA can also prevent apoptosis by inhibiting mROS formation.[35] In the KEGG enrichment analysis, the cAMP signaling pathway was up-regulated, and the relative expression of CREB mRNA increased. Therefore, whether dioscin can induce the survival and proliferation of thyroid cells by upregulating the cAMP/PKA/CREB signaling pathway deserves further study. Furthermore, it remains to be explored whether dioscin can balance the survival and proliferation of thyroid cells induced by the cAMP/PKA/CREB pathway with the simultaneous inhibition of cell proliferation and autophagy induced by mTOR.

Conclusion

In conclusion, this study suggests that dioscin can improve the expression of T3, T4, FT3, FT4, and TSH hormones in AIT model rats and can down-regulate the levels of TGAb, TPOAb and TRAb and thereby alleviating the pathological processes and inflammatory response involving the thyroid gland, activities that may be attributed to the inhibition of mTOR and TLR4/NF-κB signaling pathways.

Abbreviations

AIT, autoimmune thyroiditis; T3, triiodothyronine; T4, thyroxine; FT3, free triiodothyronine; FT4, free thyroxine; TSH, thyroid stimulating hormone; TgAb, thyroglobulin antibody; TPOAb, thyroid peroxidase antibody; TRAb, thyrotropin receptor antibody; ELISA, enzyme-linked immunosorbent assay; RT-PCR, reverse transcription-polymerase chain reaction; IHC-P, immunohistochemistry; NF-κB, nuclear factor kappa B; mTOR, mechanistic target of rapamycin; TLR4, toll-like receptor 4; PTg, porcine thyroglobulin; CFA, freund's complete adjuvant; IFA, incomplete adjuvant; mROS, mitochondrial ROS.

Data Sharing Statement

Sequencing data for this study can be found in online repositories. The names of the repository/repositories and accession number(s) can be found below: https://www.ncbi.nlm.nih.gov/sra/PRJNA930657.

Ethical Approval and Informed Consent

All experimental procedures were approved by the Laboratory Animal Ethics Committee of Beijing University of Chinese Medicine according to the Guideline for Ethical Review of Animal Welfare (GB/T 35892–2018).

Author Contributions

All authors made a significant contribution to the work reported, whether that is in the conception, study design, execution, acquisition of data, analysis and interpretation, or in all these areas; took part in drafting, revising or critically

reviewing the article; gave final approval of the version to be published; have agreed on the journal to which the article has been submitted; and agree to be accountable for all aspects of the work.

Funding

Disclosure

The authors report no conflicts of interest in this work.

References

1. Buzdugă CM, Costea CF, Dumitrescu GF, et al. Cytological, histopathological and immunological aspects of autoimmune thyroiditis: a review. *Rom J Morphol Embryol*. 2017;58(3):731–738.
2. Fan Y, Xu S, Zhang H, et al. Selenium supplementation for autoimmune thyroiditis: a systematic review and meta-analysis. *Int J Endocrinol*. 2014;2014:904573. doi:10.1155/2014/904573
3. McLeod DSA, Cooper DS. The incidence and prevalence of thyroid autoimmunity. *Endocrine*. 2012;42(2):252–265. doi:10.1007/s12020-012-9703-2
4. Hasham A, Tomer Y. Genetic and epigenetic mechanisms in thyroid autoimmunity. *Immunol Res*. 2012;54(1–3):204–213. doi:10.1007/s12026-012-8302-x
5. Cui L, Yang G, Ye J, et al. Dioscin elicits anti-tumour immunity by inhibiting macrophage M2 polarization via JNK and STAT3 pathways in lung cancer. *J Cell Mol Med*. 2020;24(16):9217–9230. doi:10.1111/jcmm.15563
6. Tao X, Yin X, Xu L, Peng J. Dioscin: a diverse acting natural compound with therapeutic potential in metabolic diseases, cancer, inflammation and infections. *Pharmacol Res*. 2018;137:259–269. doi:10.1016/j.phrs.2018.09.022
7. Zhang Y, Xu Y, Qi Y, et al. Protective effects of dioscin against doxorubicin-induced nephrotoxicity via adjusting FXR-mediated oxidative stress and inflammation. *Toxicology*. 2017;378:53–64. doi:10.1016/j.tox.2017.01.007
8. Yongjun C, Nan Q, Yumeng S, Xiaowen J, Weibo W. Dioscin alleviates hashimoto's thyroiditis by regulating the SUMOylation of IRF4 to promote CD4+CD25+Foxp3+ treg cell differentiation. *Autoimmunity*. 2021;54(1):51–59. doi:10.1080/08916934.2020.1855428
9. Xu XG, Zhang H, Bi XL, Gu J, Shi YL, Hou Q. Xiaoyin recipe for psoriasis induces a Th1/Th2 balance drift toward Th2 in peripheral blood mononuclear cells of experimental autoimmune thyroiditis rats. *Chin J Integr Med*. 2012;18(2):137–145. doi:10.1007/s11655-012-0995-0
10. Bolger AM, Lohse M, Usadel B. Trimmomatic: a flexible trimmer for Illumina sequence data. *Bioinformatics*. 2014;30(15):2114–2120. doi:10.1093/bioinformatics/btu170
11. Kim D, Langmead B, Salzberg SL. HISAT: a fast spliced aligner with low memory requirements. *Nat Methods*. 2015;12(4):357–360. doi:10.1038/nmeth.3317
12. Roberts A, Trapnell C, Donaghey J, Rinn JL, Pachter L. Improving RNA-Seq expression estimates by correcting for fragment bias. *Genome Biol*. 2011;12(3):R22. doi:10.1186/gb-2011-12-3-r22
13. Trapnell C, Williams BA, Pertea G, et al. Transcript assembly and quantification by RNA-Seq reveals unannotated transcripts and isoform switching during cell differentiation. *Nat Biotechnol*. 2010;28(5):511–515. doi:10.1038/nbt.1621
14. Anders S, Pyl PT, Huber W. HTSeq–a Python framework to work with high-throughput sequencing data. *Bioinformatics*. 2015;31(2):166–169. doi:10.1093/bioinformatics/btu638
15. Anders S, Huber W. Differential expression analysis for sequence count data. *Genome Biol*. 2010;11(10):R106. doi:10.1186/gb-2010-11-10-r106
16. Kanehisa M, Araki M, Goto S, et al. KEGG for linking genomes to life and the environment. *Nucleic Acids Res*. 2008;36(Database issue):D480–484. doi:10.1093/nar/gkm882
17. Langmead B, Salzberg SL. Fast gapped-read alignment with Bowtie 2. *Nat Methods*. 2012;9(4):357–359. doi:10.1038/nmeth.1923
18. Roberts A, Pachter L. Streaming fragment assignment for real-time analysis of sequencing experiments. *Nat Methods*. 2013;10(1):71–73. doi:10.1038/nmeth.2251
19. Panos GD, Boeckler FM. Statistical Analysis in Clinical and Experimental Medical Research: simplified Guidance for Authors and Reviewers. *Drug Des Devel Ther*. 2023;17:1959–1961. doi:10.2147/DDDT.S427470
20. Sl C, Y J, S L. Iodine Intake Increases IP-10 Expression in the Serum and Thyroids of Rats with Experimental Autoimmune Thyroiditis. *Int J Endocrinol*. 2014;2014. doi:10.1155/2014/581069
21. Liu H, Li Y, Zhu Y, Ma L, Xue H. Notch Signaling Pathway Promotes Th17 Cell Differentiation and Participates in Thyroid Autoimmune Injury in Experimental Autoimmune Thyroiditis Mice. *Mediators Inflamm*. 2023;2023:1195149. doi:10.1155/2023/1195149
22. Wang W, Zhang BT, Jiang QL, et al. Leptin receptor antagonist attenuates experimental autoimmune thyroiditis in mice by regulating Treg/Th17 cell differentiation. *Front Endocrinol (Lausanne)*. 2022;13:1042511. doi:10.3389/fendo.2022.1042511
23. Guo Q, Qu H, Zhang H, Zhong X, Prunella Vulgaris L. Attenuates Experimental Autoimmune Thyroiditis by Inhibiting HMGB1/TLR9 Signaling. *Drug Des Devel Ther*. 2021;15:4559–4574. doi:10.2147/DDDT.S325814
24. Yang X, Chen L, Zhao L, et al. Cordyceps sinensis-derived fungus Isaria felina ameliorates experimental autoimmune thyroiditis in mice. *Biomed Pharmacother*. 2021;140:111733. doi:10.1016/j.biopha.2021.111733
25. Peng S, Sun X, Wang X, et al. Myeloid related proteins are up-regulated in autoimmune thyroid diseases and activate toll-like receptor 4 and pro-inflammatory cytokines in vitro. *Int Immunopharmacol*. 2018;59:217–226. doi:10.1016/j.intimp.2018.04.009
26. Aktaş T, Celik SK, Genc GC, Arpaci D, Can M, Dursun A. Higher Levels of Serum TLR2 and TLR4 in Patients with Hashimoto's Thyroiditis. *Endocr Metab Immune Disord Drug Targets*. 2020;20(1):118–126. doi:10.2174/1871530319666190329114621
27. Zhang HL, Lin YH, Qu Y, Chen Q. The effect of miR-146a gene silencing on drug-resistance and expression of protein of P-gp and MRP1 in epilepsy. *Eur Rev Med Pharmacol Sci*. 2018;22(8):2372–2379. doi:10.26355/eurrev_201804_14829

28. Liu Q, Rehman H, Krishnasamy Y, Lemasters JJ, Zhong Z. Ischemic preconditioning attenuates acute lung injury after partial liver transplantation. *Int J Physiol Pathophysiol Pharmacol*. 2018;10(2):83–94.

29. Strickland I, Ghosh S. Use of cell permeable NBD peptides for suppression of inflammation. *Ann Rheum Dis*. 2006;65(Suppl 3):iii75–82. doi:10.1136/ard.2006.058438

30. Liu H, Tian Q, Ai X, et al. Dihydroartemisinin attenuates autoimmune thyroiditis by inhibiting the CXCR3/PI3K/AKT/NF-κB signaling pathway. *Oncotarget*. 2017;8(70):115028–115040. doi:10.18632/oncotarget.22854

31. Dunlop EA. Tee AR. mTOR and autophagy: a dynamic relationship governed by nutrients and energy. *Semin Cell Dev Biol*. 2014;36:121–129. doi:10.1016/j.semcdb.2014.08.006

32. Chen D, Huang X, Lu S, et al. miRNA-125a modulates autophagy of thyroiditis through PI3K/Akt/mTOR signaling pathway. *Exp Ther Med*. 2019;17(4):2465–2472. doi:10.3892/etm.2019.7256

33. Schmitz F, Heit A, Dreher S, et al. Mammalian target of rapamycin (mTOR) orchestrates the defense program of innate immune cells. *Eur J Immunol*. 2008;38(11):2981–2992. doi:10.1002/eji.200838761

34. Morshed SA, Ma R, Latif R, Davies TF. How one TSH receptor antibody induces thyrocyte proliferation while another induces apoptosis. *J Autoimmun*. 2013;47:17–24. doi:10.1016/j.jaut.2013.07.009

35. Morshed SA, Davies TF. Graves' Disease Mechanisms: the Role of Stimulating, Blocking, and Cleavage Region TSH Receptor Antibodies. *Horm Metab Res*. 2015;47(10):727–734. doi:10.1055/s-0035-1559633